# Intrinsic and Extrinsic Electron Trapping in $SiO_2$

Al-Moatasem El-Sayed,[1,*] Matthew B. Watkins,[1,†] Valery V. Afanas'ev,[2,‡] and Alexander L. Shluger[1,§]

[1]*Department of Physics and Astronomy and London Centre for Nanotechnology, University College London, Gower Street, London, WC1E 6BT, United Kingdom*

[2]*Department of Physics, University of Leuven, Celestijnenlaan 200D, 3001 Leuven, Belgium*

Using *ab initio* calculations we demonstrate that extra electrons in pure amorphous $SiO_2$ can be trapped in deep band gap states. Classical potentials were used to generate amorphous silica models and density functional theory to characterize the geometrical and electronic structures of trapped electrons. Extra electrons can trap spontaneously on pre-existing structural precursors in amorphous $SiO_2$ and produce $\approx 3.2$ eV deep states in the band gap. These precursors comprise wide ($\geq 132^\circ$) O–Si–O angles and elongated Si–O bonds at the tails of corresponding distributions. The electron trapping in amorphous silica structure results in an opening of the O–Si–O angle (up to almost $180^\circ$). We estimate the concentration of these electron trapping sites to be $\approx 4 \times 10^{19}$ $cm^{-3}$. The structure of these centers is similar to that of Ge and Li electron centers in $\alpha$-quartz.

PACS numbers: 71.23.An,71.55.Jv,72.15.Rn

## I. INTRODUCTION

The mechanisms of electron and hole trapping in $SiO_2$ and the nature of trapping sites are important for our understanding of a wide range of physical phenomena, such as radiation-induced damage and electrical breakdown, and for applications in fiber optics and microelectronics. In particular, electron trapping is known to have dramatic effect on the performance and reliability of electronic devices employing $SiO_2$ as gate insulator and charge trap flash memory devices.[1,2] Hole trapping in silica has been relatively well understood with the models of self-trapped holes[3–6] and several hole trapping defects well established.[7–9] However, identifying sites responsible for electron trapping in silica, bulk and surface, has proved particularly challenging. This is because of a large number of possible charge redistribution channels and presence of water and impurities in most samples. So far, the dominant electron traps have been associated with impurity-related centers, in particular, the hydrogen-related network fragments.[10–13] It has been well established that electrons can be trapped by Ge impurities substituting for Si in both $\alpha$-quartz[14] and in a-$SiO_2$[15] with models of these centers recently revisited by Griscom.[16] A defect consisting of an extra electron trapped at a four-coordinated silicon atom and stabilized by an adjacent interstitial Li ion has been observed in quartz.[17]

However, little is still known regarding the possibility of *intrinsic* electron trapping in the a-$SiO_2$ network. Bersuker *et al.* used molecular models to suggest that electrons can be trapped by Si–O bonds in a-$SiO_2$ leading to their weakening thus facilitating Si–O bond dissociation.[18] Further calculations by Camellone *et al.* have shown that electrons can be trapped in non-defective continuum random network model of a-$SiO_2$.[19] Recent calculations have also demonstrated that the two dominant neutral paramagnetic defects at surfaces of a-$SiO_2$, the non-bridging oxygen center and the silicon dangling bond, are deep electron traps and can form the corresponding negatively charged defects.[20] However, these theoretical predictions have not yet been confirmed experimentally due to challenges in identifying defect centers.

Unlike in optical fibers and other optical devices, where electrons and holes are created by electronic excitation, in metal-oxide-semiconductor (MOS) devices they are often injected from Si substrate. For example, electron trapping at an energy of 2.8 eV below the conduction band of a-$SiO_2$ has been observed using photon-stimulated tunneling experiments in device-grade oxides grown on Si and SiC crystals in a series of papers.[21–24] Further low-temperature capacitance[25] and Hall effect measurements[26,27] on 4H-SiC MOS devices revealed that the density of these electron trapping states can be as high as $10^{14}$ $cm^{-2}$ $eV^{-1}$. The trap density of $10^{13}$ $cm^{-2}$ measured inside a 2-nm thick near-interface $SiO_2$ layer [21,24] corresponds to $\approx 5 \times 10^{19}$ $cm^{-3}$ in terms of volume concentration. This is much higher than observed densities of the established intrinsic defects in thermally grown a-$SiO_2$. The absence of a comparable density of electron traps in bulk a-$SiO_2$ and the strong sensitivity of electron trapping to the incorporation of nitrogen at the interface,[28,29] suggest that electron trapping at 2.8 eV deep centers takes place not on pre-existing defects but rather in the oxide network itself. Whether the substrate plays any role in stabilizing these traps remains unclear.

In this paper we show that electrons can be trapped in a continuous non-defective a-$SiO_2$ network forming deep electron states in the gap, expanding on the results presented in our previous paper and contextualising these results within the scope of electron trapping defects in $SiO_2$.[30] The geometric structure of these centers is similar to that of electrons trapped by Ge impurities in a-$SiO_2$,[31] where the key to the electron trapping is the wide opening of the O–Ge–O angle, or Li centers in quartz where it is facilitated by the opening of the O–Si–O angle. It turns out that the precursor Si sites with wide enough O–Si–O angles naturally present in a-$SiO_2$ structure can facilitate spontaneous electron trapping at these sites.

Using this *fingerprint* we estimate the concentration of intrinsic electron trapping sites in a-$SiO_2$.

## II. DETAILS OF CALCULATION

### A. Classical calculations

The calculations presented in this work make use of both classical force-fields and *ab initio* theory. The ReaxFF[32] force-field was used to generate 20 models of amorphous $SiO_2$ each containing 216 atoms. ReaxFF was parametrized to reproduce the properties of various silica polymorphs, small silica clusters and silicon polymorphs.[33] This force-field allows one to calculate Si and O atoms in varying oxidation states based on the instantaneous geometry, which is particularly important for modeling $Si/SiO_2$ interfaces. This is accomplished by assigning a charge dependent atomic energy and exploiting the electronegativity equalization principle.[34] We used this force-field in this work with a view to studying the effect of the Si and SiC substrate in future studies.

The more extended bulk silica structures used in this study, containing between 8,640 to 401,760 atoms, were generated using the BKS potential.[35] This Buckingham-type potential parametrized for $SiO_2$ allows one to perform calculations much faster and is more suited for creating large a-$SiO_2$ structures. As we show below, comparing results obtained with two very different force-fields gives more confidence in our predictions. All classical atomistic simulations were performed using the LAMMPS code.[36]

To generate amorphous structures, molecular dynamics simulations were run using ReaxFF or BKS to melt and quench crystalline $SiO_2$ structures into an amorphous state in a manner similar to previous calculations.[37–39] Starting from supercells with a $\beta$-cristobalite structure, the system was equilibrated at 300 K and pressure of 1 atm. Maintaining the pressure at 1 atm, the temperature was linearly ramped to 5000 K (for the ReaxFF simulations) or 7000 K (for the BKS simulations). The temperature was maintained at 5000 K/7000 K for 40 ps and then brought down to 0 K at a rate of 8 K/ps. The resulting structure was then characterized by calculating basic geometrical properties, such as bond lengths, bond angles, density and total structure factor. The calculated Si–O bond lengths of the ReaxFF structures average at 1.58 Å, while the O–Si–O angles average at 109° and the Si–O–Si angles average at 155°. Densities of the ReaxFF a-$SiO_2$ structures ranged from 2.05 to 2.20 g $cm^{-3}$, averaging at 2.13 g $cm^{-3}$. Total structure factors were also calculated and showed three sharp peaks at 1.58 Å, 2.54 Å and 3.09 Å. Geometrical characterization of the structures indicates that the bond lengths are underestimated with the ReaxFF [33] while the Si–O–Si bond angles are slightly overestimated.

### B. Density Functional Theory calculations

Density functional theory (DFT), implemented in the CP2K code,[40] was used to further optimize geometries of these structures and calculate their electronic structures. The non-local Heyd, Scuseria-Ernzerhof (HSE) functional[41] was used in all calculations. Inclusion of the Hartree-Fock exchange provides an accurate description of the band gap and the localized states that may be involved in charge trapping processes. The CP2K code uses a Gaussian basis set with an auxiliary plane-wave basis set.[42] Employing Gaussian basis set has the advantage that this allows one to use fast analytical integration schemes, developed in quantum chemical methods, to calculate most of the Kohn-Sham matrix elements. The use of an auxiliary plane wave basis set allows one to use fast Fourier transform algorithms for rapid convergence of the Hartree terms. The Gaussian basis set employed for all atoms was a double-$\zeta$ basis set[43] in conjunction with the Goedecker-Teter-Hutter (GTH) pseudopotential.[44] The exception to this was for the calculation of hyperfine interactions, where the basis sets with contraction schemes of (8831/831/1) and (8411/411/11) were used for silicon[45] and oxygen,[46] respectively. The plane wave cut-off was set to 5440 eV.

To reduce the computational cost of non-local functional calculations, the auxiliary density matrix method (ADMM) was employed.[47] The density is mapped onto a much sparser Gaussian basis set than the one employed in the rest of the calculation. This allows the Hartree-Fock exchange terms, the bottleneck of a typical non-local functional calculation, where the computational expense scales to the fourth power of the number of basis functions, to be calculated much faster.

All geometry optimizations were calculated using the BFGS optimizer to minimize forces on atoms to within 37 pN. The ReaxFF structures were initially optimized in the neutral charge state. Characterizing the geometrical properties shows a slight change in the structures obtained with ReaxFF. The Si–O bond lengths after DFT optimization average at 1.62 Å while the Si–O–Si angles and the O–Si–O angles average at 147° and 109°, respectively. The calculated total structure factors showed three sharp peaks with averages at 1.61 Å, 2.62 Å and 3.09 Å, in better agreement with experiment than the ReaxFF structures. The electronic structure calculations predicted the one-electron band gap of 8.9 eV averaged over the twenty a-$SiO_2$ structures.

## III. RESULTS OF CALCULATIONS

### A. Electron trapping in $\alpha$-quartz

To better appreciate the common features of extrinsic and intrinsic electron localization in $\alpha$-quartz and in amorphous silica, it is instructive to start from the two known cases where the extra electron localization is facil-

itated by impurities. The first case concerns the electron trapping by Ge impurities substituting for Si in both $\alpha$-quartz[14] and in a-$SiO_2$.[15] The models of these centers have been recently reviewed by Griscom,[16] The cluster calculations by Pacchioni *et al.* of this so-called Ge electron center have demonstrated that a four-coordinated Ge atom in silica can trap an electron. This is accompanied by an orthorhombic distortion of the pseudo-tetrahedral Ge center which results in two short and two long Ge–O bonds.[48] The periodic DFT calculations by Du *et al.* have demonstrated that, in addition to the elongation of two Ge–O bonds, the O–Ge–O angle between the two elongated Ge–O bonds opens from about 110° to 170° to accommodate the extra electron.[31] This results from the repulsion between the localized electron and two neighboring oxygen ions.

Jani *et al.* studied the effect of a Li impurity in $\alpha$-quartz. Li impurities in quartz are present in the form of alkali-metal ions, specifically as an $[AlO_4/Li]^0$ center. A Li electron center in quartz was formed by a two-step irradiation process. The first irradiation step was performed at 150-300 K to move the Li away from its Al counterpart[49]. The second step performed after cooling the quartz sample down to 77 K formed a $[SiO_4/Li]^0$ center. The ESR spectrum of this center shows a splitting of 0.09 mT from a $^7$Li and 40.47 mT from a $^{29}$Si. This defect center is stable below 180 K and has been characterized by Jani *et al.* as an extra electron trapped at a four-coordinated Si site with an adjacent $Li^+$ ion providing stability. This model has been supported by early molecular cluster calculations of Wilson *et al.*,[50] but no other calculations have been carried out to establish the structure of this center.

We performed calculations of the Li center in $\alpha$-quartz using DFT implemented in the CP2K code. A Li atom was introduced into a 3x3x3 supercell of $\alpha$-quartz and the geometry of the system was optimized in the neutral charge state. The Li atom occupies an interstitial position in the $\alpha$-quartz lattice and no electron transfer was observed. We then investigated whether perturbing the lattice could induce electron transfer from the Li atom to Si ions. Opening an O–Si–O angle in a manner similar to the O–Ge–O described above and relaxing the structure results in the electron localization on the perturbed O–Si–O angle, as shown in Fig. 1. The relaxed structure has an extended O–Si–O angle of 150° while the Li ion is located 2.62 Å away from the Si center, bound to the two O neighbors which are not associated with the O–Si–O angle opening. The spin density of the system in Fig. 1 shows that the unpaired spin is mostly localized on the Si atom (in the open O–Si–O angle) and its two oxygen neighbors. Mulliken population analysis of the system reveals that the Li species has the charge of +0.49 $|e|$ of while the Si at the center of the wide O–Si–O angle has a Mulliken charge of +1.1 $|e|$. The Mulliken charge of Si ions in quartz is +1.43 $|e|$, indicating that the Si has gained charge. The Li stabilized electron center is 0.28 eV lower in energy than the Li interstitial atom in $\alpha$-quartz.

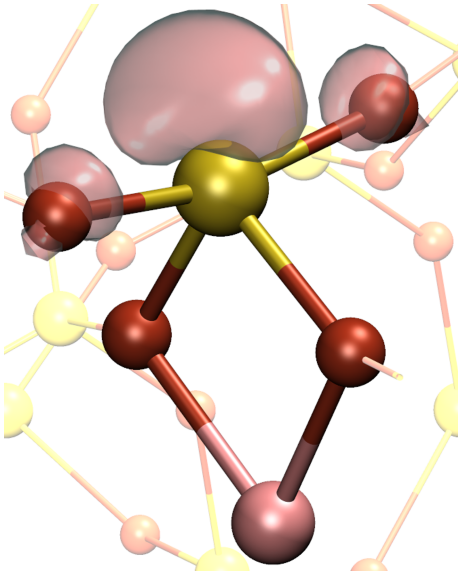

FIG. 1: (Color online) Structure and spin density distribution of the Li center in $\alpha$-quartz. The Si atoms are the larger four-coordinated lighter spheres, O atoms are the smaller, darker two-coordinated spheres and the Li ion is the large, light-coloured sphere between two O atoms. The spin density is mainly localized on the Si atom in the center. The Li ion is bound to two bridging oxygens with an O-Li-O angle of 84°. The iso-value of spin density is equal to 0.015.

These results demonstrate that the electron is localized on the Si ion in the wide O–Si–O angle. The $Li^+$ species is stabilized by the interaction with the lone pairs on the oxygen neighbors. The occupied one-electron state of the unpaired electron is located 3.1 eV below the bottom of the quartz conduction band. Moving the Li ion 7.4 Å away from the localized electron increases the total energy of the system by 0.87 eV due to the stabilizing Coulomb interaction between the electron and $Li^+$ and the weak Li-O bonding interactions. The calculated hyperfine splittings due to the interaction of the unpaired electron with the surrounding nuclei are shown in Table I and compared with the experimental results by Jani *et al.*.[17] The largest hyperfine splitting is on the Si ion, with an isotropic hyperfine splitting of 43.07 mT, with smaller hyperfine splittings on the Li and O neighbors. The good agreement of the experimental and calculated EPR parameters gives confidence that our methods are capable of reliably predicting electron localization.

We note that a common feature of both models is that the electron localization on Ge and Si ion is accompanied by an energy gain, elongation of two metal-oxide bonds and a significant opening of the –O–(Ge)Si–O– angle. This begs the question as to whether electron trapping in $\alpha$-quartz could also take place intrinsically, i.e. unaided by impurities. Previous calculations, in molecular cluster models with an $\alpha$-quartz structure, indicate that electron trapping in $\alpha$-quartz does not occur spontaneously.[48]

| Signal | Theor. | Expt.[17] |
|---|---|---|
| $a_{iso}$ Si | 43.07 | 40.47 |
| $a_{iso}$ Li | 0.11 | 0.09 |
| Principal values | 0.089 | 0.088 |
| | 0.096 | 0.098 |
| | 0.16 | 0.15 |
| g tensor | 1.995 166 | 1.998 99 |
| | 2.001 56 | 2.000 74 |
| | 2.001 94 | 2.001 66 |

TABLE I: Hyperfine splittings and principle values of the hyperfiine tensor (in mT) and the g-tensor of the Li electron trap in $\alpha$-quartz. The experimental values of hyperfine interactions for the Li-doped quartz are shown for comparison.

An extra electron was added in the perfect $\alpha$-quartz structure and the geometry optimized within DFT. The extra electron stays fully de-localized at the bottom of the conduction band and there is no change in the lattice structure. We investigated whether perturbations to the quartz structure could lead to trapping of an electron. Opening a single O–Si–O angle from 110° to 153° and optimizing the structure leads to the extra electron localization with the O–Si–O angle extending to 161°. The two Si–O bonds associated with the angle opening elongate from 1.61 Å to 1.74 Å, while the other two bonds of the tetrahedron elongate to 1.69 Å. This structural relaxation is similar to the one observed for both Ge and Li electron centers and reduces the total energy of the system by 2.50 eV. The localized electron creates a state 2.5 eV below the bottom of the $\alpha$-quartz conduction band, which is principally Si and O 'sp' in character. Mulliken population analysis reveals that the Si ion, on which the electron is localized, has charge of +1.04 $|e|$, which is significantly lower than +1.43 $|e|$ average charge of Si in $\alpha$-quartz. We note that the electron state in the Li electron center is lower by about 0.6 eV due to the Coulomb interaction with the nascent Li ion.

We have estimated the smallest O–Si–O angle opening required for trapping an electron and the corresponding energy barrier. The O–Si–O angle was increased from 109° by 2° increments and the geometry of the simulation cell was fully optimized. Opening the O–Si–O angle to 141° leads to the electron localization. The energy barrier to open a O–Si–O angle from (109.5°) to 141° is 2.5 eV.

These results demonstrate that impurity-induced or thermally activated perturbation of the quartz lattice may lead to stable electron localization on one Si(Ge) ion. Below we demonstrate that amorphous silica structure includes structural motifs which can serve as precursors for spontaneous or thermally activated electron localization on four-coordinated Si ions.

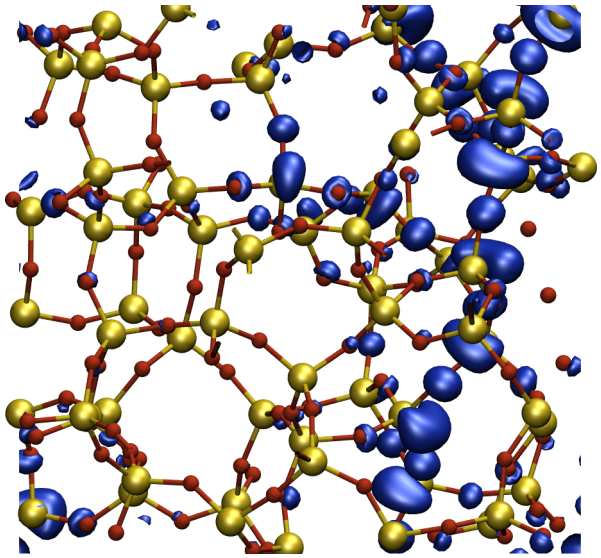

FIG. 2: (Color online) The square modulus of the wavefunction of an extra electron occupying the lowest state at the bottom of the conduction band of a-$SiO_2$. The bigger spheres connected to four atoms are Si atoms and the smaller spheres connected to two atoms are O atoms. The darker blobs represent the magnitude of the modulus of the wavefunction. The isovalue used to represent the square modulus of the wavefunction is 0.0005.

### B. Electron trapping in amorphous $SiO_2$

Electron trapping in a-$SiO_2$ was studied using twenty periodic 216 atom models of bulk a-$SiO_2$. The geometries of the ReaxFF generated amorphous structures were optimized using CP2K and then extra electron was added in each model. The extra electron initially occupies a state at the bottom of the a-$SiO_2$ conduction band. In all structures, this state is partially localized on several Si and O ions, as illustrated in Fig. 2 for one of the structures. The geometry of the system was then optimized with the extra electron, which resulted in strong electron localization in four out of the twenty models. This localization was accompanied by a local distortion around a single $SiO_4$ tetrahedron, similar to the Ge and Li electron center relaxation in $\alpha$-quartz. In each of the four structures, the extra electron localized on one Si ion with the two oxygen neighbors repelled so that an O–Si–O angle is opened from $\approx 125°$ to $\approx 172°$, as shown in Fig. 3. The Si–O bonds making up this O–Si–O angle elongated from 1.63 Å and 1.64 Å to 1.78 Å and 1.82 Å, respectively (see Fig. 3). The Mulliken population analysis shows that, as a result of the electron localization, the Si ion charge decreases by about 0.25 $|e|$. The average gain in energy resulting from the electron localization in the four models is 1.5 eV with the electron state occupied by the extra electron located at $\approx 3.17 \pm 0.05$ eV below the bottom of the $SiO_2$ conduction band, indicating a deep electron trap.

The calculated values of the hyperfine splitting induced

by the localized electron are shown in Table II. The strongest hyperfine interaction is with the Si ion, however, there is a significant interaction with the nearby oxygen atoms. Interestingly, some of the hyperfine interaction values are similar to those for the E′ center in amorphous silica. This is not surprising considering the strong electron localization on one Si ion.

In all four cases we observe that the Si ion, on which the electron traps spontaneously, forms the widest O–Si–O angle in the sample exciding 132°. In other sixteen a-$SiO_2$ samples, where the distribution of O–Si–O angles was slightly narrower, the extra electron remained delocalized in static DFT calculations. To test this further, we introduced perturbations to make two other random O–Si–O angles the widest in two separate systems. An angle in one of the systems was increased from 120.3° to 132.1°. An extra electron added into this system became localized on the Si ion within the changed angle and causes it to open further to 160.68°. An angle in a separate system was changed from 121.3° to 132.0°. When the electron was added to this system, the O–Si–O angle opened to 164.5°. These results demonstrate that a wide O–Si–O bond angle serves as a very efficient precursor to electron trapping in amorphous silica. Further calculations indicate that creating a precursor fluctuation (i.e. opening an O–Si–O angle from an average value of 120° to ≈ 133°) requires less than 0.5 eV and is within the reach of thermal fluctuations. These results also make apparent the link between geometric structure of a trap and its electronic properties and allow one to use the criterion of wide O–Si–O angle as a *fingerprint* for identifying precursor sites for spontaneous electron localization in initial a-$SiO_2$ structure and estimating the concentration of such sites, as discussed below.

| Atom | Bond length/Å | Values / mT |
|---|---|---|
| Si | | -50.98 |
| | | -45.45 |
| | | -45.23 |
| O | 1.82 | -4.181 |
| | | -2.660 |
| | | -2.624 |
| O | 1.78 | -5.714 |
| | | -4.357 |
| | | -4.298 |
| O | 1.70 | -1.548 |
| | | -1.216 |
| | | -1.212 |
| O | 1.70 | -1.581 |
| | | -1.264 |
| | | -1.259 |

TABLE II: Geometrical parameters and the average principal values of the hyperfine tensor the electron trap in a-$SiO_2$ from the four models. The bond lengths shown are with respect to the Si atom on which the electron is trapped.

### C. Finding the defect concentration

As explained above, by analysing a-$SiO_2$ sample for the presence of O–Si–O angles exceeding 132° one can estimate the potential density of electrons which could be trapped in the sample. The results from the twenty models of a-$SiO_2$ sampled indicate that the presence in the structure of an O–Si–O angle exceeding 132° always leads to spontaneous localization of extra electrons in a-$SiO_2$. This angle is at the tail of the O–Si–O angle distribution in regular $SiO_2$ structures.

To test whether the existence of these precursor sites and their concentration depends on the model of amorphous structure and to obtain better statistics, we constructed three additional samples of amorphous $SiO_2$ using the BKS interatomic potentials[35] as described in section II. These potentials are often used in studying properties of a-$SiO_2$ and give structural parameters in good agreement with experimental data.[37–39] The three samples have dimensions of $50 \times 25 \times 5$ nm$^3$, $25 \times 12.5 \times 2.5$ nm$^3$, and $12.5 \times 7 \times 1.5$ nm$^3$ and include 401,760, 55,296, and 8,640 atoms, respectively. We searched these models for the O–Si–O angle exceeding the critical value of 132° to estimate the concentration of electron trapping precursor sites. The concentration of electron trapping sites in all the a-$SiO_2$ models proved to be the same and equal to $\approx 4 \times 10^{19}$cm$^{-3}$. It is interesting to note that, in spite of the difference in size and force-field used, this concentration agrees well with our original observation of four trapping sites in twenty 216 atom samples. This linear scaling demonstrates the universal nature of the precursor site.

## IV. DISCUSSION AND CONCLUSIONS

Our calculations demonstrate qualitatively similar character of extra electron localization in both crystalline and amorphous $SiO_2$. In $\alpha$-quartz, a substitutional Ge atom provides a local perturbation which facilitates the localization of an extra electron at the Ge site. A Li atom in $\alpha$-quartz donates an electron to a neighboring Si ion and further stabilizes the defect state by the Coulomb potential. In both cases, the electron localization on Ge and Si ions is facilitated by the opening of the O-Si(Ge)-O angle. The electron localization in pure bulk $\alpha$-quartz requires opening O–Si–O angle from 109° to ≈141°, but introducing this distortion costs ≈ 2.5 eV.

In amorphous silica the statistical distribution of geometrical properties leads to existence of precursor Si sites, which can spontaneously trap an electron in a state which is ≈ 3.2 eV below the bottom of the conduction band. The estimated concentration of these precursor sites is $\approx 4 \times 10^{19}$ cm$^{-3}$. The relatively large average distance between precursor sites suggests that diffusion

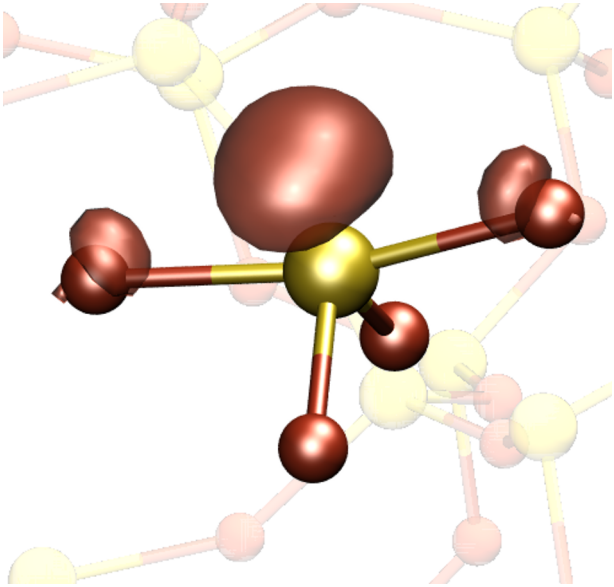

FIG. 3: (Color online) The atomic structure and spin density distribution of an intrinsic electron trap in a-$SiO_2$. We highlight the $SiO_4$ tetrahedron and show the spin density only on the nearest ions. The spin density isovalue is 0.02.

of trapped electrons via thermally activated tunneling mechanism should be quite inefficient and they are more likely to move via thermal activation into the mobility edge states of amorphous silica at high temperature.

We note that predicting the electron and hole trapping in insulators is challenging due to the well-known self-interaction error inherent in local functionals used in most DFT calculations.[51] In this work we used the non-local functional HSE and obtained the electron localization in Ge in Li electron centers in $\alpha$-quartz. The hyperfine splitting constants and g-tensor components calculated for the Li center in quartz are in good agreement with the experimental values suggesting that HSE can predict the electronic structure of electron traps in silica relatively accurately. We recently compared the performance of HSE for studying hole trapping in monoclinic $ZrO_2$ with the cancellation of nonlinearity method, which ensures the elimination of self-interaction and obtained very similar results.[52,53] Therefore we are fairly confident in our predictions of electron trapping in $\alpha$-quartz and a-$SiO_2$. The calculated hyperfine splittings for the trapped electron are close to those attributed to E′ type centers in silica.[54] This means that, in spite of a potentially high concentration of electron trapping sites, identifying these electron traps experimentally using EPR in bulk a-$SiO_2$ samples may be challenging.

We correlate these states to electron traps identified experimentally in MOS devices[55] at an energy of 2.8 eV below the conduction band of a-$SiO_2$ grown on Si and SiC crystals.[21–24] These electron traps have initially been correlated with oxygen deficient centers at the near-interfacial oxide.[22,23,29] However, later experiments on nitridated SiC/$SiO_2$ samples questioned this attribution, particularly when taking into account the fact that the density of known O-deficiency centers ($E'_\gamma$ and $E'_\delta$ centers) rarely approaches the density range of $10^{13}cm^{-2}$ found for the 2.8 eV deep electron traps. Although these electron traps are especially pronounced in 4H-SiC/$SiO_2$ devices, they seem to play a role in all devices containing $SiO_2$ as the insulating material, suggesting that they can be intrinsic to the oxide. For instance, these traps are expected to appear below the conduction band of Si nanocrystals in the case of quantum confinement.[56,57]

We suggest that the intrinsic electron traps in a-$SiO_2$ discussed in this work could be good candidates for understanding these data. The calculated concentration of the electron traps approaches the experimentally observed value for the states filled by direct tunneling from semiconductor substrate or photo-stimulated tunnelling from $SiO_2$ valence band. Populating such a density of electron traps via electron injection from an electrode through the $SiO_2$ conduction band should be much less efficient because an electron capture requires dissipating about 1.5 eV of relaxation energy into phonons during the trapping process. This process is likely to be less efficient than fast electron transport in the conduction band of thin oxide towards an opposite electrode, but can take place in bulk oxide. The observed trap energy at 2.8 eV is between the values calculated for $\alpha$-quartz (2.5 eV) and a-$SiO_2$ (3.2 eV). Our results indicate that the geometry of the oxide structure can significantly affect the position of the defect level, and the discrepancy between the experimental value and our a-$SiO_2$ value may reflect the higher oxide density in thermally grown oxides[58,59] rather than the density obtained in this work.

To summarize, our results demonstrate that, similar to holes,[3] electrons can be trapped at structural precursor sites in an amorphous silica matrix, forming deep electron states in the oxide bandgap. These states can be responsible for the electron trapping observed at interfaces of $SiO_2$-based MOS devices and should be present in bulk silica samples.

## V. ACKNOWLEDGEMENTS

The authors acknowledge EPSRC and the EU FP7 project MORDRED (EU Project grant No. 261868) for financial support. We are grateful to A. Kimmel, M. Wolf, G. Bersuker, A. Stesmans, T. Grasser, B. Kaczer and F. Schanovsky for useful and stimulating discussions. We would like to thank the UK's HPC Materials Chemistry Consortium, which is funded by EPSRC (EP/F067496), for providing computer resources on the UK's national high-performance computing service HECToR.

* Electronic address: al-moatasem.el-sayed.10@ucl.ac.uk
† Electronic address: matthew.watkins@ucl.ac.uk
‡ Electronic address: valeri.afanasiev@fys.kuleuven.be
§ Electronic address: a.shluger@ucl.ac.uk

[1] D. M. Fleetwood, S. T. Pantelides, and R. D. Schrimpf, eds., *Defects in microelecronic materials and devices* (CRC Press, 2009).
[2] T. Y. Chan, K. K. Young, and C. Hu, IEEE Elect. Dev. Lett. **8**, 93 (1987).
[3] D. L. Griscom, J. Non-Cryst. Solids **352**, 2601 (2006).
[4] G. Pacchioni and A. Basile, Phys. Rev. B **60**, 9990 (1999).
[5] A. V. Kimmel, P. V. Sushko, and A. L. Shluger, J. Non-Cryst. Solids **353**, 599 (2007).
[6] S. Sicolo, G. Palma, C. Di Valentin, and G. Pacchioni, Phys. Rev. B **76**, 075121 (2007).
[7] L. Skuja, J. Non-Cryst. Solids **239**, 16 (1998).
[8] G. Pacchioni, L. Skuja, and D. L. Griscom, eds., *Defects in $SiO_2$ and Related Dielectrics: Science and Technology* (Nato Science Series, 2000).
[9] D. L. Griscom, Physics Research International **2013** (2013).
[10] E. H. Nicollian, C. N. Berglund, P. F. Schmidt, and J. M. Andrews, J. Appl. Phys. **42**, 5654 (1971).
[11] A. Hartstein and D. R. Young, Appl. Phys. Lett. **38**, 631 (1981).
[12] V. V. Afanas'ev, J. M. M. de Nijs, P. Balk, and A. Stesmans, J. Appl. Phys. **78**, 6481 (1995).
[13] V. V. Afanas'ev and A. Stesmans, Appl. Phys. Lett. **71**, 3844 (1997).
[14] J. Isoya, J. A. Weil, and R. F. C. Claridge, J. Chem. Phys. **69**, 4876 (1978).
[15] D. L. Griscom, J. Non-Cryst. Solids **357**, 1945 (2011).
[16] D. L. Griscom, Opt. Mater. Express **1**, 400 (2011).
[17] M. G. Jani, L. E. Halliburton, and A. Halperin, Phys. Rev. Lett. **56**, 1392 (1986).
[18] G. Bersuker, A. Korkin, Y. Jeon, and H. Huff, Appl. Phys. Lett. **80**, 832 (2002).
[19] M. Farnesi Camellone, J. C. Reiner, U. Sennhauser, and L. Schlapbach, Phys. Rev. B **76**, 125205 (2007).
[20] L. Giordano, P. V. Sushko, G. Pacchioni, and A. L. Shluger, Phys. Rev. Lett. **99**, 136801 (2007).
[21] V. V. Afanas'ev and A. Stesmans, Phys. Rev. Lett. **78**, 2437 (1997).
[22] V. V. Afanas'ev and A. Stesmans, Appl. Phys. Lett. **70**, 1260 (1997).
[23] V. V. Afanas'ev and A. Stesmans, Microelectron. Eng. **36**, 149 (1997).
[24] V. V. Afanas'ev and A. Stesmans, J. Phys.: Condens. Matter **9**, L55 (1997).
[25] V. V. Afanas'ev, A. Stesmans, M. Bassler, G. Pensl, and M. J. Schulz, Appl. Phys. Lett. **76**, 336 (2000).
[26] N. S. Saks and A. K. Agarwal, Appl. Phys. Lett. **77**, 3281 (2000).
[27] N. S. Saks, S. S. Mani, and A. K. Agarwal, Appl. Phys. Lett. **76**, 2250 (2000).
[28] V. V. Afanas'ev, A. Stesmans, F. Ciobanu, G. Pensl, K. Y. Cheong, and S. Dimitrijev, Appl. Phys. Lett. **82**, 568 (2003).
[29] V. V. Afanasev, F. Ciobanu, S. Dimitrijev, G. Pensl, and A. Stesmans, J. Phys.: Condens. Matt. **16**, S1839 (2004).
[30] A. -M. El-Sayed, M. B. Watkins, A. L. Shluger, and A. V. V., Microelectron. Engineering **109**, 68 (2013).
[31] J. Du, L. R. Corrales, K. Tsemekhman, and E. J. Bylaska, Nucl. Instrum. Meth. B **255**, 188 (2007).
[32] A. C. T. van Duin, A. Strachan, S. Stewman, Q. Zhang, X. Xu, and W. Goddard, J. Phys. Chem. A **107**, 3803 (2003).
[33] J. C. Fogarty, H. M. Aktulga, A. Y. Grama, A. C. T. van Duin, and S. A. Pandit, J. Chem. Phys. **132**, 174704 (2010).
[34] R. T. Sanderson, *Chemical Bonds and Bond Energy* (Academic press, 1976).
[35] B. W. H. van Beest, G. J. Kramer, and R. A. van Santen, Phys. Rev. Lett. **64**, 1955 (1990).
[36] S. Plimpton, J. Comp. Phys. **117**, 1 (1995).
[37] S. Mukhopadhyay, P. V. Sushko, A. M. Stoneham, and A. L. Shluger, Phys. Rev. B **70**, 195203 (2004).
[38] A. Roder, W. Kob, and K. Binder, J. Chem. Phys. **114**, 7602 (2001).
[39] K. Vollmayr, W. Kob, and K. Binder, Phys. Rev. B **54**, 15808 (1996).
[40] J. VandeVondele, M. Krack, F. Mohamed, M. Parrinelo, T. Chassaing, and J. Hutter, Comp. Phys. Comm. **167**, 103 (2005).
[41] J. Heyd, G. E. Scuseria, and M. Ernzerhof, J. Chem. Phys. **124**, 219906 (pages 1) (2006).
[42] G. Lippert, J. Hutter, and M. Parrinello, Mol. Phys. **92**, 477 (1997).
[43] J. VandeVondele and J. Hutter, J. Chem. Phys. **127**, 114105 (2007).
[44] S. Goedecker, M. Teter, and J. Hutter, Phys. Rev. B **54**, 1703 (1996).
[45] B. Civalleri and P. Ugliengo, J. Phys. Chem. B **104**, 519 (2000).
[46] M. D. Towler, N. L. Allan, N. M. Harrison, V. R. Saunders, W. C. Mackrodt, and E. Apra, Phys. Rev. B **50**, 5041 (1994).
[47] M. Guidon, J. Hutter, and J. VandeVondele, J. Chem. Theory Comput. **8**, 2348 (2010).
[48] G. Pacchioni and C. Mazzeo, Phys. Rev. B **62**, 5452 (2000).
[49] M. E. Markes and L. E. Halliburton, J. Appl. Phys. **50**, 8172 (1979).
[50] T. M. Wilson, J. A. Weil, and P. S. Rao, Phys. Rev. B **34**, 6053 (1986).
[51] J. L. Gavartin, P. V. Sushko, and A. L. Shluger, Phys. Rev. B **67**, 035108 (2003), ISSN 1098-0121.
[52] K. P. McKenna, M. J. Wolf, A. L. Shluger, S. Lany, and A. Zunger, Phys. Rev. Lett. **108**, 116403 (2012).
[53] M. J. Wolf, K. P. McKenna, and A. L. Shluger, J. Phys. Chem. C **116**, 25888 (2012).
[54] M. G. Jani, R. B. Bossoli, and L. E. Halliburton, Phys. Rev. B **27**, 2285 (1983).
[55] I. Pintilie, C. M. Teodorescu, F. Moscatelli, R. Nipoti, A. Poggi, S. Solmi, L. S. L. vlie, and B. G. Svensson, J. Appl. Phys. **108**, 024503 (2010).
[56] V. V. Afanas'ev and A. Stesmans, Phys Rev. B **59**, 2025 (1999).
[57] G. Seguini, S. Schamm-Chardon, P. Pellegrino, and M. Perego, Appl. Phys. Lett. **99**, 082107 (2011).
[58] A. C. Diebold, D. Venables, Y. Chabal, D. Muller, M. Weldon, and E. Garfunkel, Mater. Sci. Semicond. Process. **2**,

103 (1999).
[59] A. Waseda and K. Fujii, IEEE Trans. Instrum. Meas. **56**, 628 (2007).